JCTC Journal of Chemical Theory and Computation

Article

pubs.acs.org/JCTC

Intermediate Hamiltonian Fock Space Multireference Coupled Cluster Approach to Core Excitation Spectra

Achintya Kumar Dutta,† Jitendra Gupta,† Nayana Vaval, and Sourav Pal*

Physical Chemistry Division, CSIR-National Chemical Laboratory, Pune 411008, India

Supporting Information

ABSTRACT: The Fock space multireference coupled cluster (FSMRCC) method provides an efficient approach for the direct calculation of excitation energies. In intermediate Hamiltonian (IH-FSMRCC) formulation, the method is free from intruder state problems and associated convergence difficulties, even with a large model space. In this paper, we demonstrate that the IH-FSMRCC method with suitably chosen model space can be used for the accurate description of core excitation spectra of molecules, and our results are in excellent agreement with the experimental values. We have investigated the effect of choice of model space on the computed results. Unlike the equation-of-motion (EOM)-based method, the IH-FSMRCC does not require any special technique for convergence and in singles and doubles approximation gives a performance comparable to that of the standard EOMEE-CCSD method, even better in some of the cases.

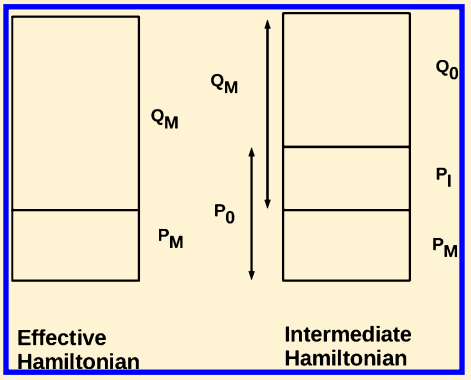

1. INTRODUCTION

X-ray absorption spectroscopy (XAS) has emerged as an important tool for elucidation of structure of different materials in recent times. The XAS is generally characterized by excitation of electron from the core into the virtual orbitals. Depending upon the nature of the excitation, the XAS is divided into two broad categories. The first one is the near edge X-ray absorption fine structure (NEXAFS), i.e., absorption taking place within the bound states and low-energy resonances in the continuum. The second category includes the extended X-ray absorption fine structure (EXAFS), where the ejected electron is well above the ionization continuum. In present time, XAS, NEXAFS, and EXAFS have been routinely used[1] in elucidation of structure, composition, and electronic distribution of surfaces, soft-condensed matter,[2] and environmental chemistry.

The proper understanding and accurate interpretation of experimental data often require reliable theoretical description of the phenomenon. However, theoretical description of core excitation spectra is difficult. The large relaxation effect accompanying the excitation of core electron into the valence or Rydberg state often makes a balanced description of ground and core-excited state a complicated one.[3]

Several theoretical approaches have been defined in the literature for the computation of core excitation spectra, such as X_α methods,[4] transition state and transition potential methods,[5−7] self-consistent field methods (ΔSCF),[5] density functional theory and its time-dependent analogues (TD-DFT),[6−11] the static exchange approach (STEX),[6] and configuration interaction (CI) methods.[7,8] There also exists Green function-based methods[9] and algebraic diagrammatic construction (ADC) approaches,[10,11] which offer an efficient way to calculate core excitation energy as direct difference of energy.

The accurate simulation of core excitation spectra requires a balanced description of both correlation and relaxation effects. The coupled cluster-based approaches,[12−14] which have been extremely successful in describing valence excitation spectra, can be useful for the purpose. The existing coupled cluster (CC) approaches to core excitation processes, namely, the open-shell electron attachment equation-of-motion coupled cluster (OS-EA-EOMCC) method[3] or its SAC-CI analogue (OS-SAC-CI),[15] separate the orbital relaxation processes from the correlation effects and predict core excitation spectra in reasonable agreement with experimental values.[16] However, both methods have the problem of solving the coupled cluster equation for core-ionized reference. Similar convergence problems also occur for solving the coupled cluster equation for maximum overlap method (MOM)-based coupled cluster methods.[17] Moreover, Norman and co-workers[18] have shown that within the single-reference coupled cluster framework, only the single and doubles approximation is not enough for quantitatively correct core excitation energy, and inclusion of higher-order excitations is crucial for accurate treatment of the relaxation effects associated with core-level excitation. Recently, Kowalski and co-workers[19] have shown that the state-specific multireference coupled cluster (SS-MRCC) method,[20,21] even in singles and doubles approximation, can give accurate core excitation spectra and the method is free from the convergence difficulties associated with the standard single-reference coupled cluster methods for core excitation spectra. Mukherjee and co-workers[22] have shown promising results using unitary

Received: April 3, 2014
Published: August 19, 2014

   dx.doi.org/10.1021/ct500285e | J. Chem. Theory Comput. 2014, 10, 3656−3668

group approach (UGA)-based MRCC methods[23,24] for core-ionization and core excitation spectra. However, both state-specific and UGA-based MRCC requires two separate calculations for the ground and the excited states.[25] On the other hand, direct difference of energy-based MRCC approaches calculate the excitation energy in a single calculation and can be used as an efficient way for calculation of core excitation energy. The Fock space multireference coupled cluster (FSMRCC) method[26−31] is well-known for its ability to give an accurate difference of energies such as ionization potential, electron affinity, and excitation energy. Despite the great success achieved for valence-excited spectra,[32,33] FSMRCC in the standard effective Hamiltonian formulation is difficult to apply for core excitation spectra, mainly due to the intruder state[34−38] problem, which leads to convergence difficulties in large active space calculations. This problem is not only restricted to the FSMRCC method and is inherent to any multireference effective Hamiltonian theory. Malrieu et. al.[39] was the first to introduce the intermediate Hamiltonian (IH) approach, in the context of quasi-degenerate perturbation theory, as an efficient way to bypass the intruder state problem. Different groups have persuaded various IH schemes. Kaldor and co-worker's[40,41] formulation of IH in FSMRCC method leads to an altogether new method. On the other hand, the IH method proposed by Meissner[42−49] leads to identical results as that of the effective Hamiltonian formulation of FSMRCC. The eigenvalue-independent partitioning (EIP) technique[50] by Mukherjee and co-workers also leads to a specific implementation of IH in Fock space.

In the IH formulation, the FSMRCC method (IH-FSMRCC)[49,51−56] is free from intruder state problem and can be used to calculate multiple roots with a large active space in a single calculation. Bartlett and co-workers[32,43,44,51−54] have used IH-FSMRCC method for the prediction of valence excitation spectra, with great success. The aim of this paper is to investigate the performance of IH-FSMRCC method for the simulation of core excitation spectra.

The paper is organized as follows: the Section 2 contains a brief discussion on the theory of IH-FSMRCC and computational strategies for the calculation of core excitation spectra. Numerical results and discussion on them are followed in Section 3. The concluding remarks are found in Section 4.

2. THEORY AND COMPUTATIONAL DETAILS

All MRCC theories can be classified into two broad categories: the first one describes a specific root, known as the state-specific MRCC, and the other is the multiroot description by effective Hamiltonian approach.

Various approaches are available for describing the state-specific MRCC ansatz, such as Brillouin−Wigner (BW) MRCC ansatz,[20,57] the state-specific ansatz suggested by Mukherjee and co-workers (MK-MRCC),[21,58−61] exponential multireference wave function ansatz (MR expT)[62,63] and internally contracted multireference coupled cluster ansatz (ic-MRCC).[64]

On the other hand, effective Hamiltonian-based theories are subdivided into two basic subclasses: Hilbert space (HS) approach and Fock Space (FS) approach. In both the approaches, energies are obtained by diagonalization of the effective Hamiltonian defined within a prechosen model space, and both approaches are fully size extensive. The HS-MRCC approach[65,66] uses a state universal operator with different cluster operators for each determinant in the model space. The FS-MRCC approach, on the other hand, uses common vacuum and a valence universal wave operator, which correlates model space with the virtual space. The HSMRCC method is more suitable for the calculation of potential energy surface. On the other hand, the FSMRCC method is more suitable for direct difference of energy calculation such as ionization potential, electron affinity, and excitation energies. In this paper, we have used the FSMRCC method for the calculation of core excitation energies.

2.1. Effective Hamiltonian Formulation of FSMRCC Theory. The FSMRCC is based on the concept[27,67] of a common vacuum, which is generally, but not necessarily, an N electron closed shell Hartree−Fock determinant. The holes and the particles are defined with respect to this common vacuum. These holes and particles are further classified into active and inactive ones. The model space is then constructed by a linear combination of suitably chosen (based on energetic criteria) active configurations. Thus, a model space for a (p,h) valence Fock space, which includes h active hole and p active particle, can be written as

$$\left|\psi_{(0)\mu}^{(p,h)}\right\rangle = \sum_i C_{i\mu}^{(p,h)} \left|\phi_\mu^{(p,h)}\right\rangle \tag{1.1}$$

The principal idea of effective Hamiltonian theory is to extract some selective eigenvalues of Hamiltonian from the whole eigenvalue spectrum. To fulfill the purpose, the configuration space is partitioned into model space and orthogonal space. When all possible resulting configurations, generated by distributing the valence electrons among all the valence orbitals in all possible ways, are included in the model space, it is referred to as complete model space (CMS). An incomplete model space (IMS) results when only a subset of these configurations is included. The projection operator for model space is defined as

$$P_M^{(p,h)} = \sum_i \left|\Phi_i^{(p,h)}\right\rangle \left\langle \Phi_i^{(p,h)}\right| \tag{1.2}$$

The projection operator in the orthogonal space, i.e., the virtual space, is defined as

$$Q_M = 1 - P_M \tag{1.3}$$

The diagonalization of the effective Hamiltonian takes care of the nondynamic correlation coming from the interactions of the model space configurations. Whereas, the dynamic correlation arises due to the interactions of the model-space configurations with the virtual space configurations. This interaction is introduced through a universal wave operator Ω, which is parametrized such that it generates the exact wave function by acting on the model space. To generate the exact states for the (p,h) valence system, the wave operator must be able to generate all the valid excitations from the model space. The valence universal wave operator Ω has the form

$$\Omega = \{e^{\tilde{S}^{(p,h)}}\} \tag{1.4}$$

Where, the braces indicate normal ordering of the cluster operators, and $\tilde{S}^{(p,h)}$ is defined as following

$$\tilde{S}^{(p,h)} = \sum_{k=0}^{p} \sum_{l=0}^{h} \hat{S}^{(k,l)} \tag{1.5}$$

The cluster operator $\tilde{S}^{(k,l)}$ is capable of destroying exactly k active particles and l active holes, in addition to creation of holes and particles. The $\tilde{S}^{(p,h)}$ subsumes all lower sector Fock

space $\tilde{S}^{(k,l)}$ operators. The $\tilde{S}^{(0,0)}$ is equivalent to standard single-reference coupled cluster amplitudes.

The Schrödinger equation for the manifold of quasi-degenerate states can be written as

$$\hat{H}|\Psi_i^{(p,h)}\rangle = E_i|\Psi_i^{(p,h)}\rangle \tag{1.6}$$

The correlated μ^{th} wave function in MRCC formalism can be written as

$$|\Psi_\mu^{(p,h)}\rangle = \Omega|\Psi_{(0)\mu}^{(p,h)}\rangle \tag{1.7}$$

From eq 1.1 we get

$$\hat{H}\Omega(\sum_i C_{i\mu}^{(p,h)}\phi_i^{(p,h)}) = E_\mu\Omega(\sum_i C_{i\mu}^{(p,h)}\phi_i^{(p,h)}) \tag{1.8}$$

The effective Hamiltonian for (p,h) valence system can be defined as

$$\sum_j (\hat{H}_{\text{eff}}^{(p,h)})_{ij} C_{j\mu} = E_\mu C_{i\mu} \tag{1.9}$$

where

$$(\hat{H}_{\text{eff}}^{(p,h)})_{ij} = \langle\phi_i^{(p,h)}|\Omega^{-1}\hat{H}\Omega|\phi_j^{(p,h)}\rangle \tag{1.10}$$

Equation 1.10 can be written as

$$\hat{H}_{\text{eff}} = P_M^{(p,h)}\Omega^{-1}\hat{H}\Omega P_M^{(p,h)} \tag{1.11}$$

However, the Ω^{-1} may not be well-defined in all the cases.[67] Therefore, the above definition of effective Hamiltonian is seldom used. Instead, the Bloch−Lindgren approach is generally used for solving the equations. The Bloch equation is just a modified form of Schrödinger equation.

$$\hat{H}\Omega P_M = \Omega\hat{H}_{\text{eff}}P_M \tag{1.12}$$

The Bloch-Lindgren approach eliminates the requirement of Ω^{-1} for the solution of effective Hamiltonian.

The Bloch projection approach to solve the equation involves left projection of eq 1.12 with P and Q, leading to

$$P_M^{(k,l)}[\hat{H}\Omega - \Omega\hat{H}_{\text{eff}}]P_M^{(k,l)} = 0 \tag{1.13}$$

$$Q_M^{(k,l)}[\hat{H}\Omega - \Omega\hat{H}_{\text{eff}}]P_M^{(k,l)} = 0 \tag{1.14}$$

$$; \forall\ k = 0, ..., p;\ l = 0, ..., h$$

To solve the equations, an additional normalization is imposed through parametrization of Ω. In case of CMS, this is generally performed by imposing the intermediate normalization condition $P_M\Omega P_M = P_M$. However, the situation is a little bit different in case of incomplete model space. Mukherjee[68] has shown that in case of incomplete model space, the valence universality of the wave operator is sufficient to guarantee linked-cluster theorem; however, one need to relax the intermediate normalization. Pal et al.[29] have shown that for the special case of quasi-complete model space in (1,1) sector, the intermediate normalization can be used without any loss of generality.

In general, the equations for Ω and H_{eff} are coupled to each other through eqs 1.13 and 1.14 and H_{eff} cannot be expressed explicitly in terms of Ω. However, when intermediate normalization is imposed, H_{eff} can directly be written as a function of Ω. In this case, eq 1.13 can be written as

$$P_M^{(p,h)}\hat{H}\Omega P_M^{(p,h)} = P_M^{(p,h)}\hat{H}_{\text{eff}}^{(p,h)}P_M^{(p,h)} \tag{1.15}$$

After solving the equations for Ω and H_{eff}, the diagonalization of the effective Hamiltonian within the P space gives the energies of the corresponding states and the left and the right eigenvectors.

$$\hat{H}_{\text{eff}}^{(p,h)}C^{(p,h)} = C^{(p,h)}E \tag{1.16}$$

$$\tilde{C}^{(p,h)}\hat{H}_{\text{eff}}^{(p,h)} = E\tilde{C}^{(p,h)} \tag{1.17}$$

$$\tilde{C}^{(p,h)}C^{(p,h)} = C^{(p,h)}\tilde{C}^{(p,h)} = 1 \tag{1.18}$$

The contractions among different cluster operators within the exponential are avoided due to the normal ordering, leading to partial hierarchical decoupling of cluster equations, i.e., once the amplitude equations of a particular sector of Fock space is solved, it appears as a known parameter in the equations for a higher sector of Fock space. This is commonly referred to as subsystem embedding condition (SEC). The lower valence cluster equations are decoupled from the higher valence cluster equations, because of the SEC. Hence, the Bloch equations are solved progressively from the lowest valence (0,0) sector upward up to (p,h) valence sector.

2.2. Intermediate Hamiltonian Formulation of FSMRCC Theory. In this paper, we follow the approach used by Meissner[42] to describe the IH formulation of FSMRCC. The H_{eff} is defined in the P space, with a dimension much smaller (say m) than the actual Hamiltonian. The diagonalization of the effective Hamiltonian produces m eigenvalues, which are equal to a subset of the eigenvalues of the exact Hamiltonian $\hat{H}$. When the model space configurations (P) are not energetically well separated from those of complementary space (Q), this results in a very small or negative energy denominator in the iterative solution procedure leading to divergence or severe convergence problem. It is known as intruder state problem and is a common difficulty associated with all multiroot theories. They are particularly common in complete model space treatments because such spaces include high-energy multiple excitation model spaces, which contribute very little to the wave functions, but are required for the completeness of the model space.

The IH approach overcomes the intruder state problem by introducing a buffer space between the model space and rest of the Q space. Basically, in the IH formulation, the configuration space is divided into three subspaces, namely, main, intermediate, and outer space (see Figure 1) with the projection operators P_M, P_I, and Q_0, respectively.[39,69] The main space of IH formulation is the same as the model space of effective Hamiltonian theory, while the intermediate space (P_I) has been obtained from a subpart of the complementary space (Q_M) of the effective Hamiltonian theory, by further dividing it into two parts: the intermediate and the outer space. The diagonalization of the IH provides the eigenvalues, a subset of which corresponds to those obtained through effective Hamiltonian theory. The remaining eigenvalues are essentially arbitrary.

Because of the arbitrariness of the extra solution by IH approach, the IH and its determining equations are not unique. Different variants of IH approach, employing different auxiliary conditions for the definition of IH,[41,42,50] have been proposed and applied in the context of FSMRCC. The similarity transformation approach[42] by Meissner is particularly con-

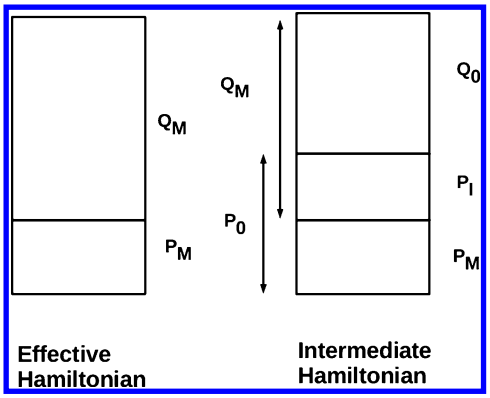

Figure 1. Model space of effective and intermediate Hamiltonian theory.

venient among them. In this formulation, the final working equation of FSMRCC can be rewritten as

$$P_I^{(p,h)}(\bar{H}\{e^{-S}\} - \{e^{-S}\}H_{\text{eff}}^{(p,h)})P_M^{(p,h)} \tag{1.19}$$

$$\hat{H}_{\text{eff}}^{(p,h)} = P_M^{(p,h)}\bar{H}\{e^{S}\}P_M^{(p,h)} \tag{1.20}$$

Let us define a new operator

$$\hat{X} = \{e^{S} - 1\}P_M \tag{1.21}$$

For, which

$$\hat{X} = Q_M\hat{X}P_M \tag{1.22}$$

and

$$\hat{X}^2 = 0 \tag{1.23}$$

Now, eqs 1.19 and 1.20 can be written in terms of $\hat{X}$ as

$$P_I^{(p,h)}(1 - \hat{X})\bar{H}(1 + X)P_M^{(p,h)} = 0 \tag{1.24}$$

$$P_M^{(p,h)}(1 - \hat{X})\bar{H}(1 + \hat{X})P_M^{(p,h)} = \hat{H}_{\text{eff}}^{(p,h)} \tag{1.25}$$

Equation 1.24 is a quadratic equation in $\hat{X}$ and, therefore, has multiple solutions. This procedure also suffers from the convergence difficulties caused by the intruder state problem. In the IH formulation, these difficulties can be averted, by splitting the similarity transformation described in eq 1.24, as follows

$$(1 - \hat{X})\bar{H}(1 + \hat{X}) = (1 - \hat{Z})(1 - \hat{Y})\bar{H}(1 + \hat{Z})(1 + \hat{Y}) \tag{1.26}$$

where

$$\hat{X} = \hat{Y} + \hat{Z} \tag{1.27}$$

$$\hat{Y} = Q_0\hat{X}P_M,$$

$$\hat{Z} = P_I\hat{X}P_M \tag{1.28}$$

and

$$P_0 = P_M + P_I \tag{1.29}$$

$$Q_M = P_I + Q_0 \tag{1.30}$$

From the definition of $\hat{X}$, $\hat{Y}$, and $\hat{Z}$

$$(1 - \hat{X}) = (1 + \hat{X})^{-1},$$

$$(1 - \hat{Y}) = (1 + \hat{Y})^{-1}, \text{ and}$$

$$(1 - \hat{Z}) = (1 + \hat{Z})^{-1} \tag{1.31}$$

From the above relation, it is clear that if eq 1.24 is satisfied, then the m number of roots can be extracted equivalently both from diagonalization of $(1 - \hat{X})\bar{H}(1 + \hat{X})$ or $(1 - \hat{Y})\bar{H}(1 + \hat{Y})$ operator within the P_0 to P_0 space, as both operators are related to each other by a similarity transformation with respect to a third operator $(1 + Z)$.

Now the IH is defined as,

$$\hat{H}_I^{(p,h)} = P_0^{(p,h)}(1 - Y)\bar{H}(1 + Y)P_0^{(p,h)} \tag{1.32}$$

As P_M, P_I, and Q_0 are projection operators of mutually orthogonal spaces, the IH in eq 1.32 can be expressed as

$$\begin{aligned}\hat{H}_I^{(p,h)} &= P_0^{(p,h)}\bar{H}(1 + \hat{Y})P_0^{(p,h)} \\ &= P_0^{(p,h)}\bar{H}P_0^{(p,h)} + P_0^{(p,h)}\bar{H}\hat{Y}P_M^{(p,h)}\end{aligned} \tag{1.33}$$

Now, for solving the above equation, we assume that equations for (0,0) sector, which is essentially the standard closed shell single reference cluster equation, have already been solved.

Now, for (1,0) and (0,1) sectors of Fock space

$$Y^{(0,1)} = Y^{(1,0)} = 0 \tag{1.34}$$

$$X^{(0,1)} = Z^{(0,1)} = S^{(0,1)} \tag{1.35}$$

$$X^{(1,0)} = Z^{(1,0)} = S^{(1,0)} \tag{1.36}$$

For, (1,1) sector of Fock space

$$X^{(1,1)} = Y^{(1,1)} + Z^{(1,1)} \tag{1.37}$$

$$\begin{aligned}Y^{(1,1)} = Q_0^{(1,1)}\{&S_2^{(0,1)} + S_2^{(1,0)} + S_1^{(0,1)}S_2^{(1,0)} + S_1^{(1,0)}S_2^{(0,1)} \\ &+ S_2^{(0,1)}S_2^{(1,0)}\}P_M^{(1,1)}\end{aligned} \tag{1.38}$$

and

$$Z^{(1,1)} = P_I^{(1,1)}\{S_1^{(0,1)} + S_1^{(1,0)} + S_1^{(0,1)}S_1^{(1,0)} + S_2^{(1,1)}\}P_M^{(1,1)} \tag{1.39}$$

The IH for (0,1) and (1,0) sector can be written as

$$H_I^{(0,1)} = P_0^{(0,1)}\bar{H}P_0^{(0,1)} \tag{1.40}$$

and

$$H_I^{(1,0)} = P_0^{(1,0)}\bar{H}P_0^{(1,0)} \tag{1.41}$$

Now the eigenvalue problem for (0,1) and (1,0) sector can be solved by diagonalization of $\bar{H}$ within the space spanned by 1h, 2h1p and 1p, 2p1h determinants, respectively. Hence, the IHFSCC approach for one valence problem is independent of choice of active space and becomes identical with IP/EA-EOMCC approach.[70,71] However, for the solution of higher sectors, the cluster amplitudes for (0,1) and (1,0) are explicitly required. Therefore, it becomes essential to define the model space by choosing a subset of total number of holes and particles as active, which is generally, but not necessarily near the Fermi level.

The cluster amplitudes for the one valence sectors can be obtained[42,50] by imposing the intermediate normalization

Table 1. Core Excitation Energies of Water (in eV)

excitation	basis	EOMEE-CCSD	ΔUGA-SUMRCC[a]	ΔUGA-IIMS-SUMRCC[a]	UGA-QFSMRCC[a]	BW-MRCCSD[b]	MK-MRCCSD[b]	IH-FSMRCCSD[c]	experimental[d]
(1a1 → 4a1)	cc-pVDZ	538.40[a]	537.43	537.70	537.50	537.62	537.56	538.36 (10,5)	534.0
	cc-pVTZ	535.34[a]	534.15	534.40	534.15	534.34	534.94	535.50 (10.5)	
	cc-pCVTZ	XXX[e]	–	–	–	–	–	536.23 (10,5)	
	aug-cc-pVTZ	535.32	–	–	–	–	–	535.66 (20,5)	
	aug-cc-pCVTZ	XXX[e]	–	–	–	–	–	535.89 (20,5)	
(1a1 → 2b1)	cc-pVDZ	540.21[a]	539.33	539.33	539.42	539.55	539.49	540.15 (10,5)	535.9
	cc-pVTZ	537.13[a]	536.05	536.05	536.05	536.20	536.15	537.30 (10,5)	
	cc-pCVTZ	XXX[e]	–	–	–	–	–	537.66 (10,5)	
	aug-cc-pVTZ	537.11	–	–	–	–	–	537.49 (20,5)	
	aug-cc-pCVTZ	XXX[e]	–	–	–	–	–	537.65 (20,5)	

[a]Values taken from ref 22. [b]Value taken from ref 19. [c]The quantity in the bracket is the active space chosen for the calculations. [d]Values taken from refs 8, 83, and 84. [e]XXX indicates calculations have not converged.

condition on the selectively chosen eigenvectors corresponding to active holes and particles.

Now the IH for (1,1) sector is defined as

$$H_I^{(1,1)} = P_0^{(1,1)}\bar{H}P_0^{(1,1)} + P_0^{(1,1)}\bar{H}Y^{(1,1)}P_M^{(1,1)} \quad (1.42)$$

Now from eq 1.42, it can be seen that the IH for the (1,1) sector of Fock space can be constructed by the matrix representation of H_I within 1h1p space. As the expression for $Y^{(1,1)}$ does not contain $S^{(1,1)}$, the solution of the eigenvalue problem for (1,1) sector in IH framework, only requires the knowledge of lower sector amplitudes. However, $S^{(1,1)}$ can be determined by putting the intermediate normalization on the selectively chosen eigenvectors, analogous to that in one valence problem. Very recently Pal and co-workers[72] have extended the idea for calculation of properties in (1,1) sector, within the IH framework.

In this IH formulation of FSMRCC, the equations are not solved in a coupled iterative manner. Rather, the eigenvalue problem is solved through diagonalization procedure. This leads to easier convergence, even with a large active space, which not only helps one to obtain more numbers of states, but also systematically improves the correlation effects in case of (1,1) sector.

2.3. Computational Consideration. The IH formulation of FSMRCC leads to an easy and near black box way of describing the core excitation spectra within the framework of multireference coupled cluster theory. In the IH formulation of FSMRCC, the matrix diagonalization is performed within the space spanned by only 1h1p determinants. The small dimension of the final matrix leads to easier convergence in Davidson's iterative diagonalization technique,[73,74] which is not the case in equation-of-motion excitation energy (EOMEE)-CC, where the matrix diagonalization is performed over 1h1p and 2h2p space. The large dimension of the final matrix in EOMEE-CCSD leads to severe convergence problem in Davidson's iterative methodm for the excitation of core electrons, especially in large basis sets. The small dimension of the final matrix in IH-FSMRCC method even gives the scope of direct diagonalization, which is impossible in EOMEE-CC framework due to the large size of the final matrix.

The problem of slow convergence can still occur in IH-FSMRCC framework while solving the equations for one valence problem with a large active space, which is essentially the same as solving the IP/EA-EOMCC equations via Davidson's iterative technique. However, in both IP- and EA-EOMCC method, the diagonalization being a N^5 scaling method, a large number of iterations can be afforded for their solutions, which is not the case in EOMEE-CC, where the diagonalization step scales as N^6.

To test the suitability of the IH-FSMRCC method for the simulation of core excitation spectra, we have calculated the core excitation energy of H_2O, N_2, CO, CH_4, C_2H_2, H_2CO, and C_2H_4 in singles and doubles approximation (IH-FSMRCCSD) in cc-pVDZ and cc-pVTZ basis sets[75,76] and compared our results with the EOMEE-CCSD and other available theoretical methods. All the IH-FSMRCCSD calculations were performed using our in-house coupled cluster codes. The newly written IH-FSMRCCSD codes have been validated using our existing effective Hamiltonian-based FSRMCCSD codes[30,31,33,77] for the ($1a_1 \rightarrow 4a_{1)}$ core excitation of water in cc-pVDZ and cc-pVTZ basis set. In (1,5) and (2,5) active space, the intermediate and effective Hamiltonian-based FSMRCCSD codes give identical results, in both cc-pVDZ and cc-pVTZ basis set. However, the effective Hamiltonian-based code for (1,1) sector fails to converge in active space containing more than two active particles. The details of the validation are provided in Supporting Information.

The peak separations in the core excitation spectra for all the molecules are reported with respect to the lowest energy peak.

One and two electron integrals, converged Hartree−Fock coefficients, and eigenvalues were taken from GAMESS-US[78] package, and experimental geometries were used in all the cases. The EOMEE-CCSD calculations were performed using CFOUR.[79] The Cartesian coordinates of geometry used for all the molecules are provided in Supporting Information.[80]

3. RESULTS AND DISCUSSIONS

3.1. Water. The experimental photoabsorption spectra of water, as reported by Sette and co-workers,[81] are dominated by two intense peaks at 534.0 and 535.9 eV. The peak corresponds to excitation of an electron from 1s orbital ($1a_1$) of oxygen to empty 3s ($4a_1$) and 3p ($2b_1$) orbitals.

Table 1 presents the IH-FSMRCCSD values of the core excitation energies of water in different basis sets. We have

studied the core excitation energies corresponding to ($1a_1 \rightarrow 4a_1$) and ($1a_1 \rightarrow 2b_1$) transitions. The IH-FSMRCC method gives core excitation energy of 538.36 and 535.50 eV for the ($1a_1 \rightarrow 4a_1$) transition, in cc-pVDZ and cc-pVTZ basis set, respectively. The corresponding values for the ($1a_1 \rightarrow 2b_1$) transition in cc-pVDZ and cc-pVTZ basis set, are 540.15 and 537.30 eV, respectively. It can be seen that in both cc-pVDZ and cc-pVTZ basis sets, IH-FSMRCCSD values are in the same range as that of the EOMEE-CCSD values. However, the values are inferior compared to that obtained in the state-specific[19] and UGA-based[22] MRCC methods, at the same level of truncation of cluster amplitudes. The inferior performance of both IH-FSMRCC and EOMCC may be attributed to the double excitation character of the core-excited states of water, as pointed out by Norman and co-workers,[18] present in both $1a_1 \rightarrow 4a_1$ and $1a_1 \rightarrow 2b_1$ transitions of water.

Another interesting feature is the reproducibility of the experimental peak separation of 1.90 eV between the lowest two peaks. The IH-FSMRCCCSD method gives a peak separation 1.80 eV in cc-pVTZ basis set, which is in reasonable agreement with the experimental value. The EOMEE-CCSD method gives similar performance and shows a peak separation of 1.79 eV in the same basis set. All, the other multireference methods exactly reproduce the experimental peak separation of 1.90 eV, except the ΔUGA-IIMS-SUMRCC method, which shows a much smaller peak separation value 1.65 eV.

Here, it should be noted that the determination of core excitation energies in methods like MK-MRCC, BW-MRCC, UGA-SUMRCC, or UGA-IIMS-SUMRCC requires two separate calculations,[25] and at the same time significant theoretical expertise is required to perform the calculations. On the other hand, the IH-FSMRCCSD method calculates the core excitation energy corresponding to multiple transitions in a single calculation and can be used in a near "black box" way. Obviously, the ease of using the IH-FSMRCC is less than that of the EOMCC method because of active space dependency of former. However, the IH-FSMRCC is free from the convergence problem associated with the EOMEE-CCSD method for core excitation, especially in large basis sets.

Bartlett and co-workers[52,82] have highlighted the crucial importance of choice of active space in determining the quality of the results in the IH-FSMRCC method[43] or its closely related STEOMCC method.[82] We have studied the effect of active space on the core excitation energy corresponding to $1a_1 \rightarrow 2b_1$ excitation of water, as shown in Table 2. For the IH-FSMRCC calculations of core excitation energy, all the holes are taken active by default. Therefore, the choice of active space mainly depends upon the number of active virtual orbital. In the minimal active space (2,5), the core excitation energy corresponding to $1a_1 \rightarrow 2b_1$ transition is 537.64 eV. The percentage error compared to experiment is around 0.3%. However, the result improves with the increase in the active space. In an active space of (5,5), the result becomes comparable to EOMEE-CCSD results. It is difficult to define any quantitative relationship between the choice of active space and the quality of the results. However, Bartlett and co-workers[82] have proposed the magnitude of the percentage active component in any state as a qualitative measure of the quality of active space for that particular state, in the context of STEOMCC. A percentage active component below 98 would reflect that the chosen active space is insufficient for the proper inclusion of correlation effect for that specific excited state. A similar trend is observed for core excitation energy reported in Table 2. In minimal active space (5,2), where the percentage active component is only 97.60%, the IH-FSMRCC shows large deviation from experiments.[81] The result improves with the increase in percentage active component, i.e., with increase in active space and seems to converge with respect to active space at a percentage active component over 99.00%. Here, it should be noted that the threshold value of the percentage active component for the valence excitation in STEOMCC, as reported by Bartlett and co-workers,[82] was slightly less at 98%. It indicates that the simulation of core excitation spectra requires better inclusion of correlation effect than that of the valence one.

Table 2. Effect of Active Space on the Core Excitation Spectra (in eV) of Water ($1a1 \rightarrow 2b1$) Computed in IHFSMRCC Method (cc-pVTZ basis set)

active space	active component	IH-FSMRCCSD	experimetal[a]
(2,5)	96.60	537.64	535.9
(5,5)	97.53	537.33	
(6,5)	97.53	537.33	
(7,5)	97.53	537.33	
(8,5)	99.20	537.31	
(9,5)	99.27	537.30	
(10,5)	99.27	537.30	

[a]Value taken from refs 8, 83, and 84.

Basis set has a significant effect on the core excitation energy. On increasing the basis set from cc-pVDZ to cc-pVTZ, the core excitation energies, in both EOMCC and FSMRCC methods, undergo red shift and move closer to the experiment. The augmentation has negligible effect on core excitation energy. The use of core−valence correlation consistent basis set and its augmented versions lead to slight overestimation of the peak corresponding to ($1a_1 \rightarrow 4a_1$) and ($1a_1 \rightarrow 2b_1$) transitions, compared to its normal correlation consistent versions. Here it should be mentioned that the cc-pVDZ basis set results are not trustworthy. However, we have used the cc-pVDZ basis set in the present and the subsequent test cases, just to compare our IH-FSMRCC results with EOMCC results. The latter generally fails to converge in any higher basis set.

The description of the only lowest energy peaks, often the most intense one, perhaps is important for comparison between different theoretical methods. However, it is of little significance for experimental chemists. The reproduction of experimental spectra requires the core excitation energy corresponding to the transition to virtual orbitals higher than LUMO, which is of low intensity and often difficult to reproduce in standard ab initio methods. One of the most powerful features of IH-FSMRCC is that it can calculate transition from core to multiple virtual orbitals in a single calculation. We have found that only the augmented core−valence correlation consistent (aug-cc-pCVXZ) family of basis set is successful in reproducing the peak separations of these low intensity peaks. The normal correlation consistent basis sets fail to reproduce the peak corresponding to transition from core to high-lying virtual orbitals. A detailed analysis of the basis set dependency of peaks due to transition from core to virtual orbitals higher than the LUMO, is provided in the Supporting Information. However, it should be noted that even the augmented core−valence correlation consistent aug-cc-pCVXZ (X = D,T, and Q) family of basis set is also not totally adequate for the simulation of high lying core-excited Rydberg states, and they require

dx.doi.org/10.1021/ct500285e | J. Chem. Theory Comput. 2014, 10, 3656−3668

specially constructed basis set with sufficient diffused functions, which has not considered in the present study.

Table 3 presents the core excitation energies of water in a hierarchy of aug-cc-pCVXZ (X = D, T, and Q) basis set. It can be seen that the peak separations are overestimated in both IH-FSMRCCSD and EOMEE-CCSD methods in aug-cc-pCVDZ basis set. It can be seen that the extent of overestimation is slightly higher in EOMEE-CCSD method than that in IH-FSMRCCSD for all the peaks. All the peak separations decrease, on increasing the basis set from aug-cc-pCVDZ to aug-cc-pCVTZ, and they move toward experimental value. The peak separations continue to be overestimated even in IH-FSMRCCSD/aug-cc-pCVTZ level of theory, except that of between the lowest two peaks, which is slightly underestimated. However, the extent of overestimation is greatly reduced from that in aug-cc-pCVDZ. The peak separation further improves on moving to aug-cc-pCVQZ, however, the extent of improvement is less than that observed on going from aug-cc-pCVDZ to aug-cc-pCVTZ basis. The EOMEE-CCSD method, on the other hand fails to converge in both aug-cc-pCVTZ and aug-cc-pCVQZ basis set.

Table 3. Peak Separations (in eV) in the Core Excitation Spectrum of H_20

excitation	EOMEE-CCSD	IH-FSMRCCSD[a]	experimental[b]
	aug-cc-pCVDZ		
1S(1a1) → 3S(4a1)	537.15	537.61	534.00
1S(1a1) → 3P(2b2)	+2.01	+1.86	+1.90
1S(1a1) → 3P(2b1)	+4.10	+3.86	+3.0
1S(1a1) → 3P(5a1)	+4.29	+4.10	
1S(1a1) → 4S(6a1)	+4.95	+4.30	+3.8
1S(1a1) → 4P(3b2)	+5.06	+4.72	4.4
	aug-cc-pCVTZ		
1S(1a1) → 3S(4a1)	XXX[c]	535.89	534.00
1S(1a1) → 3P(2b2)		+1.76	+1.90
1S(1a1) → 3P(2b1)		+3.46	+3.0
1S(1a1) → 3P(5a1)		+3.68	
1S(1a1) → 4S(6a1)		+4.14	+3.8
1S(1a1) → 4P(3b2)		+4.27	4.4
	aug-cc-pCVQZ		
1S(1a1) → 3S(4a1)	XXX[c]	535.92	534.00
1S(1a1) → 3P(2b2)		+1.90	+1.90
1S(1a1) → 3P(2b1)		+3.33	+3.0
1S(1a1) → 3P(5a1)		+3.51	
1S(1a1) → 4S(6a1)		+3.90	+3.8
1S(1a1) → 4P(3b2)		+4.42	4.4

[a]An active space of (5,15) has been used. [b]Value taken from refs 8, 83, and 84. [c]XXX indicates calculations have not converged.

3.2. N_2. In Table 4, we report the core excitation energy corresponding to $1\sigma_g \rightarrow \pi_g$ transition for N_2 in EOMCC, IH-FSMRCC, and other multireference coupled cluster methods. In cc-pVDZ basis, the IH-FSMRCCSD method shows core excitation energy of 404.14 eV for the $1\sigma_g \rightarrow \pi_g$ transition, and it performs significantly better than the EOMEE-CCSD method. Even, it performs better than the state-specific MRCC, and UGA-based MRCC methods, on contrary to that in the case of water. An improvement in the basis set leads to betterment of the results in all the methods. The IH-FSMRCC method gives core excitation energy of 401.33 eV ($1\sigma_g \rightarrow \pi_g$ transition) in cc-pVTZ basis, which shows reasonable agreement with experimental value[83,84] of 400 eV. In cc-pVTZ basis set also, the IH-FSMRCCSD method performs better than the EOMEE-CCSD and other MRCC methods, and its performance is similar to that of the CR-EOMCCSD(T) and r-CR-EOMCCSD(T) values reported by Kowalski and co-workers.[19]

Table 5 presents the comparison of the peak separations in IH-FSMRCCSD method with that of the experimental results.

Table 5. Peak Separations (in eV) in the Core-Excitation Spectrum of N_2

excitation	EOMEE-CCSD	IH-FSMRCCSD[a]	experimental[b]
	aug-cc-pCVDZ		
$1\sigma_g \rightarrow 1\pi_g$ (π^*)	403.61	403.55	400.0
$1\sigma_u \rightarrow 4\sigma_g$ (3s)	+6.76	+6.75	+6.15
$1\sigma_g \rightarrow 2\pi_u$ (3p)	+6.82	+6.89	
$1\sigma_g \rightarrow 2\pi_u$ (3p)	+8.41	+8.51	+7.11
$1\sigma_u \rightarrow 5\sigma_g$ (3d)	+8.31	+8.40	+8.35
$1\sigma_u \rightarrow 2\pi_g$ (3d)	+9.10	+9.00	+8.63
	aug-cc-pCVTZ		
$1\sigma_g \rightarrow 1\pi_g$ (π^*)	XXX[c]	401.88	400.0
$1\sigma_u \rightarrow 4\sigma_g$ (3s)		+5.70	+6.15
$1\sigma_u \rightarrow 2\pi_u$ (3p)		+5.93	
$1\sigma_g \rightarrow 2\pi_u$ (3p)		+6.80	+7.11
$1\sigma_u \rightarrow 5\sigma_g$ (3d)		+8.15	+8.35
$1\sigma_u \rightarrow 2\pi_g$ (3d)		+8.73	+8.63
	aug-cc-pCVQZ		
$1\sigma_g \rightarrow 1\pi_g$ (π^*)	XXX[c]	402.20	400.0
$1\sigma_u \rightarrow 4\sigma_g$ (3s)		+6.40	+6.15
$1\sigma_u \rightarrow 2\pi_u$ (3p)		+6.00	
$1\sigma_g \rightarrow 2\pi_u$ (3p)		+7.17	+7.11
$1\sigma_u \rightarrow 5\sigma_g$ (3d)		+8.36	+8.35
$1\sigma_u \rightarrow 2\pi_g$ (3d)		+8.76	+8.63

[a]An active space of (7,15) has been used. [b]Values taken from ref 83. [c]XXX indicates calculations have not converged.

The separation between the peaks in the IH-FSMRCCSD/aug-cc-pCVDZ level of theory is slightly overestimated. The EOMEE-CCSD method also gives similar results and reproduces all the features of the spectra calculated at IH-FSMRCCSD/aug-cc-pCVDZ level of theory. On moving to

Table 4. Core Excitation Energies for N_2 (in eV)

excitation	basis	EOMEE-CCSD[a]	CR-EOM-CCSD(T)[b]	r-CR-EOM-CCSD(T)[b]	ΔUGA-SUMRCC[a]	UGA-QFSMRCC[a]	BW-MRCCSD[b]	MK-MRCCSD[b]	IH-FSMRCCSD[c]	experimental[d]
	cc-pVDZ	404.38	–	–	404.83	404.80	–	–	404.14 (10,7)	400 eV (with the 1.8−2.4 eV resolution)
($1\sigma_g \rightarrow \pi_g$)	cc-pVTZ	401.68	401.60	401.39	401.88	401.84	401.72	401.86	401.33 (10,7)	

[a]Values taken from ref 22. [b]Value taken from ref 19. [c]The quantity in the bracket is the active space chosen for the calculations. [d]Values taken from ref 83.

Table 6. Core Excitation Energy (in eV) for CH4(C 1S → LUMO A_1)

basis	SAC-CI[a]	ΔUGA-SUMRCC[b]	EOMEE-CCSD[b]	IH-FSMRCCSD[c]	experimental[d]
cc-pVDZ	–	–	290.84	290.26 (10,5)	287.05
cc-pVTZ	–	–	XXX[e]	288.10 (10,5)	
cc-pCVTZ	288.50	287.80	XXX[e]	287.79 (10,5)	

[a]Values taken from ref 85. [b]Value taken from ref 22. [c]The quantity in the bracket is the active space chosen for the calculations. [d]Values taken from ref 85. [e]XXX indicates calculations have not converged.

aug-cc-pCVTZ basis set, the peak separations in IH-FSMRCCSD method decrease. The peak separation values in IH-FSMRCCSD show very slight change from aug-cc-pCVTZ to aug-cc-pVQZ basis, and the values are in reasonable agreement with that of the corresponding experimental numbers. The EOMEE-CCSD method on the other hand fails to converge in both aug-cc-pCVTZ and aug-cc-pCVQZ basis sets.

3.3. CH_4. CH_4 presents an interesting test case because of its highly symmetric Td structure. Table 6 shows that in EOMEE-CCSD/cc-pVDZ level of theory, the core excitation energy corresponding to (C(1S) → LUMO (A_1)) transition is 290.84 eV, and it deviates considerably from the experimental value[85] of 287.05 eV. The IH-FSMRCCSD method provides a value of 290.26 eV in the same basis set, which shows little improvement over the EOMEE-CCSD method. However, the core excitation energy in IH-FSMRCCSD method still deviates by more than 2 eV from the experiment. Increasing the basis set from cc-pVDZ to cc-pVTZ basis set, the core excitation energy in IH-FSMRCCSD method improves and moves toward the experimental value. The core excitation energy in IH-FSMRCCSD/cc-pVTZ level of theory is 288.10 eV, which is in reasonable agreement with the experimental value[85] of 287.05 eV. On the other hand, the EOMEE-CCSD method fails to converge in cc-pVTZ basis set. The IH-FSMRCC method gives very similar performance to ΔUGA-SUMRCC values reported by Mukherjee and co-workers[22] in cc-pCVTZ basis set and gives better agreement with experiment than the SAC-CI values, reported by Ehara and Nakasuji,[85] in the same basis set. The EOMEE-CCSD calculation has not converged in cc-pCVTZ basis set.

Table 7 reports the separations of different peaks in IH-FSRMCCSD calculated core excitation spectra of CH_4. In aug-cc-pCVDZ basis set, the peak separation is overestimated compared to the experimental values, especially, the peak separation corresponding to (C (1s) → 4p (t_2)) transition is overestimated by around 1 eV. The EOMEE-CCSD method leads to a similar performance. On increasing the basis set from aug-cc-pCVDZ to aug-cc-pCVTZ, the peak separations in IH-FSMRCCSD method decrease, except that between the lowest two peaks, which remains unchanged. All the peak separations undergo very slight change from aug-cc-pCVTZ to aug-cc-pCVQZ basis set. However, the values continue to be overestimated compared to the experimental peak separations. It should be noted that all the transitions from the core orbital, except the lowest one in CH_4, have considerable double excitation character, for which (1,1) sector of FSMRCC fails to take care in a balanced way within the CCSD approximation. More over the quantitative agreement with experiment will require a more flexible basis set with sufficient diffuse functions and inclusion of relativistic effect, both which have not been considered in the present study. The EOMEE-CCSD method have the same problem of overestimation of the peaks, in addition to the fact that it fails to converge in both aug-cc-pCVTZ and aug-cc-pCVQZ basis set.

Table 7. Peak Separations (in eV) in the Core Excitation Spectrum of CH_4

excitation	EOMEE-CCSD	IH-FSMRCCSD[a]	experimental[b]
	aug-cc-pCVDZ		
C (1s) → 3s(a_1)	288.82	288.87	287.05
C (1s) → 3p(t_2)	+1.36	+1.27	+0.94
C (1s) → 3d(t_2)	+2.74	+2.76	+1.62
C (1s) → 4p(t_2)	+3.39	+3.53	+2.36
	aug-cc-pCVTZ		
C (1s) → 3s(a_1)	XXX[c]	288.12	287.05
C (1s) → 3p(t_2)		+1.27	+0.94
C (1s) → 3d(t_2)		+2.59	+1.62
C (1s) → 4p(t_2)		+3.11	+2.36
	aug-cc-pCVQZ		
C (1s) → 3s(a_1)	XXX[c]	288.15	287.05
C (1s) → 3p(t_2)		+1.45	+0.94
C (1s) → 3d(t_2)		+2.34	+1.62
C (1s) → 4p(t_2)		+2.94	+2.36

[a]An active space of (5,10) has been used. [b]Values taken from ref 85. [c]XXX indicates calculations have not converged.

3.4. CO and H_2CO. CO and formaldehyde are two prototype systems, where the two core holes are widely separated and consequently can be treated independent of each other.

The dominant features of the core excitation spectra at both oxygen and carbon K edge of carbon monoxide is given by the 1s → π^* transition positioned at 534.2[86] and 287.4 eV,[87] respectively. As seen from Table 8, the IH-FSMRCCSD method reproduces the spectral peak at both edges. The core excitation energy in IH-FSMRCCSD/cc-pVDZ level of theory, corresponding to (O (1s) → π^*) transition, is 536.80 eV, which is vastly superior compared to the EOMEE-CCSD result of 538.47 eV. However, the IH-FSMRCCSD result still deviates considerably from the experimental value of 534.2 eV. The core excitation energy in IH-FSMRCCSD method undergoes a red shift in cc-pVTZ basis and approaches toward the experimental value. The IH-FSMRCCSD/cc-pVTZ level of theory gives the core excitation energy corresponding to (O (1s) → π^*)

Table 8. Core Excitation Energies (in eV) for CO

excitation	basis	EOMEE-CCSD	IH-FSMRCCSD[a]	experimental
O(1s) → π^*	cc-pVDZ	538.47	536.80 (14,7)	534.2[b]
	cc-pVTZ	XXX	534.60 (20,7)	
C(1s) → π^*	cc-pVDZ	290.30	289.39 (14,7)	287.4[c]
	cc-pVTZ	XXX[c]	287.29 (20,7)	

[a]The quantity in the bracket is the active space chosen for the calculations. [b]Value taken from ref 86. [c]Value taken from ref 87. [d]XXX indicates calculations have not converged.

dx.doi.org/10.1021/ct500285e | J. Chem. Theory Comput. 2014, 10, 3656−3668

transition at 534.60 eV, which is in good agreement with the ROHF/EA-EOMCCSD value (534.15 eV) and QRHF/EA-EOMCCSD value (533.98 eV) of Nooijen and Bartlett[3] as well as the experimental value of 534.2 eV. The EOMEE-CCSD calculation fails to converge in cc-pVTZ basis set. Similar trend is observed for the core excitation energy corresponding to the (C (1s) → π*) transition.

The dominant feature at both carbon and oxygen K edge spectra of H_2CO is given by the 1s → π* transitions. Table 9 presents the computed and experimental results[89] for both (O(1s) → π*) and (C(1s) → π*) transition of H_2CO. In cc-pVDZ basis set, the core excitation energy values corresponding to (O(1s) → π*) and (C(1s) → π*) transition of H_2CO are overestimated in EOMCC as well as in IH-FSMRCC method. On increasing the basis set from cc-pVDZ to cc-pVTZ basis, the core excitation energies at both the edges undergo a red shift and move closer to the experiment, similar to that of CO. The EOMEE-CCSD method fails to converge in cc-pVTZ basis.

Table 9. Core Excitation Energies (in eV) for H_2CO

transition	basis	EOMEE-CCSD	IH-FSMRCCSD[a]	experimental[b]
O(1s) → π*	cc-pVDZ	534.99	534.89 (8,20)	530.8
	cc-pVTZ	XXX	531.86 (8,20)	
C(1s) → π*	cc-pVDZ	289.03	288.28 (8,20)	286.0
	cc-pVTZ	XXX[c]	286.10 (8,20)	

[a]The quantity in the bracket is the active space chosen for the calculations. [b]Value taken from ref 89. [c]XXX indicates calculations have not converged.

Tables 10 and 11 present the separation of different peaks in the core excitation spectra corresponding to oxygen hole of CO and H_2CO, respectively. The peak separations in both the molecules are generally overestimated in IH-FSMRCCSD/aug-cc-pCVDZ level of theory. Especially the peak separation corresponding to (O (1s) → 4s) transition is overestimated by more than 1 eV. The EOMEE-CCSD gives almost similar performance in aug-cc-pCVDZ basis set. With increase in the basis set from aug-cc-pCVDZ to aug-cc-pCVTZ, all the peak separations slightly decrease, except that corresponding to (O (1s) → 3s) transition. The peak separations further decrease from aug-cc-pCVTZ to aug-cc-pCVQZ basis, and in aug-cc-pCVQZ basis set shows good agreement with experimental values. The EOMEE-CCSD method fails to converge in both aug-cc-pCVTZ and aug-cc-pCVQZ basis set.

Table 10. Peak Separations (in eV) in the Core Excitation Spectrum of CO (Oxygen Core Hole)

excitation	EOMEE-CCSD	IH-FSMRCCSD[a]	experimental[b]
	aug-cc-pCVDZ		
O((1s) → π*)	537.46	537.62	534.1
O((1s) → 3s)	+4.86	+4.81	+4.7
O((1s) → 3p$_\pi$)	+6.27	+6.12	+5.7
O((1s) → 4s)	+7.99	+ 8.00	+6.8
	aug-cc-pCVTZ		
O((1s) → π*)	XXX[c]	535.94	534.1
O((1s) → 3s)		+4.81	+4.7
O((1s) → 3p$_\pi$)		+6.10	+5.7
O((1s) → 4s)		+7.69	+6.8
	aug-cc-pCVQZ		
O((1s) → π*)	XXX[c]	536.04	534.1
O((1s) → 3s)		+4.54	+4.7
O((1s) → 3p$_\pi$)		+5.90	+5.7
O((1s) → 4s)		+7.30	+6.8

[a]An active space of (7,10) has been used. [b]Values taken from ref 86. [c]XXX indicates calculations have not converged.

Table 11. Peak Separations (in eV) in the Core Excitation Spectrum of H_2CO (Oxygen Core Hole)

excitation	EOMEE-CCSD	IH-FSMRCCSD[a]	experimental[b]
	aug-cc-pCVDZ		
O((1s) → π*)	534.20	534.64	530.80
O((1s) → 3s)	+5.31	+4.80	+4.67
O((1s) → 3p)	+6.35	+5.93	+5.33
O((1s) → 4s)	+8.33	+8.0	+6.85
	aug-cc-pCVTZ		
O((1s) → π*)	XXX[c]	533.05	530.80
O((1s) → 3s)		+4.82	+4.67
O((1s) → 3p)		+5.86	+5.33
O((1s) → 4s)		+7.82	+6.85
	aug-cc-pCVQZ		
O((1s) → π*)	XXX[c]	532.26	530.8
O((1s) → 3s)		+4.46	+4.67
O((1s) → 3p)		+5.60	+5.35
O((1s) → 4s)		+7.33	+6.85

[a]An active space of (8,10) has been used. [b]Values taken from ref 89. [c]XXX indicates calculations have not converged.

Table 12 and 13 report the peak separations corresponding to the carbon core hole of CO and H_2CO. The trends in the both cases are similar to that are observed for the oxygen core hole. All the peak separations are overestimated in IH-FSMRCCSD/aug-cc-pVDZ level of theory. The EOMEE-CCSD method gives a similar performance in the same basis set. The peak separations in IHFSMRCCSD method decrease from aug-cc-pCVDZ to aug-ccpCVTZ, except the peak separation corresponding to the (C (1s) → 3s) transition, which increases slightly. The peak separations further decrease from aug-ccpCVTZ to aug-cc-pCVQZ basis, and in aug-cc-pCVQZ basis the results are in reasonable agreement with the

Table 12. Peak Separations (in eV) in the Core Excitation Spectrum of CO (Carbon Core Hole)

excitation	EOMEE-CCSD	IH-FSMRCCSD[a]	experimental[b]
	aug-cc-pCVDZ		
C((1s) → π*)	289.20	288.86	287.4
C((1s) → 3s)	+5.77	+6.16	+5.0
C((1s) → 3p$_\pi$)	+6.89	+7.24	+6.9
C((1s) → 4s)	+7.00	+ 7.32	+7.5
	aug-cc-pCVTZ		
C((1s) → π*)	XXX[c]	287.96	287.4
C((1s) → 3s)		+6.28	+5.0
C((1s) → 3p$_\pi$)		+7.35	+6.9
C((1s) → 4s)		+ 7.38	+7.5
	aug-cc-pCVQZ		
C((1s) → π*)	XXX[c]	+288.13	287.4
C((1s) → 3s)		+6.04	+5.0
C((1s) → 3p$_\pi$)		+6.91	+6.9
C((1s) → 4s)		+7.33	+7.5

[a]An active space of (7,10) has been used. [b]Values taken from ref 87. [c]XXX indicates calculations have not converged.

dx.doi.org/10.1021/ct500285e | J. Chem. Theory Comput. 2014, 10, 3656−3668

Table 13. Peak Separations (in eV) in the Core Excitation Spectrum of H_2CO (Carbon Core Hole)

excitation	EOMEE-CCSD	IH-FSMRCCSD[a]	experimental[b]
	aug-cc-pCVDZ		
C((1s) → π*)	288.08	287.63	286.0
C((1s) → 3s)	+4.48	+4.84	+4.58
C((1s) → 3p)	+5.86	+6.21	+5.66
C((1s) → 4s)	+9.00	+ 8.81	+7.39
	aug-cc-pCVTZ		
C((1s) → π*)	XXX[c]	286.86	286.0
C((1s) → 3s)		+4.95	+4.58
C((1s) → 3p)		+6.13	+5.66
C((1s) → 4s)		+ 8.50	+7.39
	aug-cc-pCVQZ		
C((1s) → π*)	XXX[c]	+286.81	286.0
C((1s) → 3s)		+5.09	+4.58
C((1s) → 3p)		+5.51	+5.66
C((1s) → 4s)		+8.33	+7.39

[a]An active space of (8,10) has been used. [b]Values taken from ref 89. [c]XXX indicates calculations have not converged.

experimental value. The EOMCC method, on the other hand, fails to converge in both aug-cc-pCVTZ and aug-cc-pCVQZ basis set.

3.5. C_2H_2 and C_2H_4. In core excitation spectra of acetylene and ethylene, the core hole remains delocalized over both the carbons.

Table 14 presents the core excitation spectra corresponding to (C (1s) → π*) transition of acetylene. In cc-pVDZ basis set,

Table 14. Core Excitation Energy (in eV) for C_2H_2(C(1S) → π*)

basis	EOMEE-CCSD	IH-FSMRCCSD[a]	experimental[b]
cc-pVDZ	288.60	288.54(10,7)	285.8
cc-pVTZ	XXX[c]	286.07(10,7)	

[a]The quantity in the bracket is the active space chosen for the calculations. [b]Value taken from ref 88. [c]XXX indicates calculations have not converged.

the EOMEE-CCSD method gives a core excitation value of 288.60 eV, which deviates considerably from the experimental value[88] of 285.8 eV. The IH-FSMRCCSD method gives rise to similar results in cc-pVDZ basis set (288.54 eV). On improving the basis set to cc-pVTZ, the peak in IH-FSMRCCSD method shows a red shift and gives a core excitation energy of 286.07 eV, which is in reasonable agreement with the experimental value of 285.8 eV. The EOMEE-CCSD method fails to converge in cc-pVTZ basis set.

The core excitation spectra of ethylene ((C (1s) → π_{b2g}) transition) shows a similar trend (Table 15). In cc-pVDZ basis set, the EOMEE-CCSD method gives core excitation energy of

Table 15. Core Excitation Energy (in eV) for C_2H_4(C(1S) → π*)

basis	EOMEE-CCSD	IH-FSMRCCSD[a]	experimental[b]
cc-pVDZ	287.50	287.41(10,8)	284.67
cc-pVTZ	XXX[c]	285.41(10,8)	

[a]The quantity in the bracket is the active space chosen for the calculations. [b]Value taken from ref 88. [c]XXX indicates calculations have not converged.

287.50 eV, which is significantly overestimated compared to the experimental value[88] of 284.67 eV. The IH-FSMRCCSD method gives rise to similar results (287.41 eV). In cc-pVTZ basis set, the core excitation energy in the IH-FSMRCCSD method shows a red shift and gives a value of 285.41 eV, which is in reasonable agreement with the experimental value of 284.67 eV. The EOMEE-CCSD method fails to converge in cc-pVTZ basis set.

Tables 16 and 17 present the peak separation in core excitation spectra of acetylene and ethylene. It can be seen that

Table 16. Peak Separations (in eV) in the Core Excitation Spectrum of C_2H_2

excitation	EOMEE-CCSD	IH-FSMRCCSD[a]	experimental[b]
	aug-cc-pCVDZ		
(C(1s) →π*)	288.29	288.17	285.81
(C(1s) → 3s)	+2.42	+2.37	2.06
(C(1s) → 3p)	+3.47	+3.45	+2.99
(C(1s) → 4s)	+ 3.59	+ 3.68	+3.99
	aug-cc-pCVTZ[d]		
(C(1s) →π*)	XXX[c]	287.06	285.81
(C(1s) → 3s)		+2.47	+2.06
(C(1s) → 3p)		+2.75	+2.99
(C(1s) → 4s)		+3.52	+3.99

[a]An active space of (7,15) has been used. [b]Values taken from ref 88. [c]XXX indicates calculations have not converged. [d]One of the diffused f function removed from carbon.

Table 17. Peak Separations (in eV) in the Core Excitation Spectrum of C_2H_4

excitation	EOMEE-CCSD	IH-FSMRCCSD[a]	experimental[b]
	aug-cc-pCVDZ		
(C(1s) → π_{b2g})	XXX[c]	287.30	284.67
(C(1s) → 3s)		+2.95	+2.57
(C(1s) → 3p)		+3.50	+3.21
(C(1s) → 4s)		+ 4.32	+4.73
	aug-cc-pCVTZ[d]		
(C(1s) → π_{b2g})	XXX[c]	285.80	284.67
(C(1s) → 3s)		+2.98	+2.57
(C(1s) → 3p)		+3.51	+3.21
(C(1s) → 4s)		+ 4.35	+4.73

[a]An active space of (8,15) has been used. [b]Values taken from ref 88. [c]XXX indicates calculations have not converged. [d]One of the diffused f functions removed from carbon.

in IH-FSMRCCSD/aug-cc-pCVDZ level of theory, the peak separation corresponding to (C (1s) → 4s transition) is underestimated compared to the experimental values, and the other two peak separations are overestimated for both molecules. The EOMEE-CCSD method gives similar performance for all three peaks. The peak separations in IH-FSMRCCSD method show very small change from aug-cc-pCVDZ to aug-cc-pCVTZ basis, except that corresponding to (C(1s) → 3p transition) in C_2H_2, which increases by 0.3 eV. The EOMEE-CCSD method fails to converge in aug-cc-pCVTZ basis set for both the molecules.

4. CONCLUSIONS

In this paper, we explored the suitability of IH-FSMRCC method for simulation of core excitation spectra. The intermediate Hamiltonian formulation of Fock space provides

dx.doi.org/10.1021/ct500285e | J. Chem. Theory Comput. 2014, 10, 3656−3668

a near black box approach for the calculation of core excitation energy and is free from the convergence problem associated with the standard EOMEE-CCSD method and effective Hamiltonian formulation of FSMRCC.

Our calculations show that the choice of active space has a prominent effect in the core excitation energy obtained in IHFSMRCC method, and a large active space is necessary for a proper inclusion of correlation effect, required to model the excitation of core electrons. The IH formulation of FSMRCC makes it free from the intruder state problem and consequently ensures smooth convergence, even with large active spaces. The percentage active component can be taken as a marker of the quality of the active space, and percentage active component above 99 is required to reach saturation of core excitation energy with respect to active space, which is higher than that required for valence excitation spectra.

The IH-FSMRCCSD method gives results with similar accuracy range as that of the EOMCC method at the same level of truncation for the test cases that we have investigated. However, the EOMCC calculations converge only in very small basis sets for the core excitations. In IH-FSMRCCSD method, the deviation of the excitation energies corresponding to transition from core to LUMO (generally the most intense one) from the experiment is around 1 eV, and maximum error obtained among the test molecules is in the case of (C (1s) → π^*) transition of H_2CO. Although, the absolute errors are much larger compared to that in valence excitation spectra, the errors in the relative sense are significantly less, only 0.3% even in the case of maximum of deviation. To get a quantitative agreement with the experiment, one needs to use a flexible basis set with sufficient diffuse function and include the relativistic effect, both of which has not been considered in the present study.

The peak separations corresponding to the transition from core to high lying virtual orbitals are found to be qualitatively reproduced in IH-FSMRCCSD method. In most of the cases, they are slightly overestimated and are found to be highly sensitive to the quality of the basis set used in the calculations. Here, it should be noted that the transitions from the core to high-lying virtual orbitals often have significant double excitation character, for which quasi complete model space of (1,1) sector of IH-FSMRCC fails to take care in an effective manner within the CCSD approximation used in the present study. The inclusion of triples or an alternate approach through higher sectors of Fock space would be required for a better description of core excitation peaks having significant double excitation character. The EOMCC method suffers from the same problem in the CCSD approximation, with the additional complication that it does not converge in any reasonable basis set.

The relative performance of IH-FSMRCCSD method for the core excitation spectra, compared to state-specific and UGA-based MRCC, is not uniform for all the test cases. For water, IH-FSMRCC gives inferior performance compared to the other MRCC methods, but for N_2 it outperforms them. The lack of enough available data in other MRCC methods makes it difficult to arrive at any firm conclusion. However, the advantage of IHFSMRCC in computing core excitation energy corresponding to multiple states in a single calculation is missing in other MRCC methods, and the feature is quite essential for effective simulation of experimental core excitation spectra.

To make a concluding statement about the relative performance of the IH-FSMRCC method, compared to EOM-CC and other MRCC methods, more rigorous benchmarking using an expanded test set of molecules and large basis sets with sufficient diffuse functions is required. The work along this line is in progress and will be reported in a future publication.

■ ASSOCIATED CONTENT

Supporting Information

Cartesian coordinates of all the molecules, detail studies on basis set effect, and details of validation of the IH-FSMRCC codes. This material is available free of charge via the Internet at http://pubs.acs.org.

■ AUTHOR INFORMATION

Corresponding Author

*E-mail: s.pal@ncl.res.in.

Author Contributions

†These authors contributed equally.

Notes

The authors declare no competing financial interest.

■ ACKNOWLEDGMENTS

The authors acknowledge the grant from CSIR XII[th] five year plan project on Multiscale Simulations of Material (MSM) and facilities of the Centre of Excellence in Scientific Computing at NCL. A.K.D thanks the Council of Scientific and Industrial Research (CSIR) for a Senior Research Fellowship. S.P. acknowledges the DST J. C. Bose Fellowship project and CSIR SSB grant towards completion of the work.

■ REFERENCES

(1) Stöhr, J. In *NEXAFS Spectroscopy*; Ertl, G., Gome, R., Mills, D. L., Eds.; Springer-Verlag: Berlin, Germany, 1996; pp 292−350.

(2) Kevin, R. W.; Matteo, C.; Bruce, S. R.; Richard, D. S.; Nilsson, A.; Pettersson, L. G. M.; Goldman, N.; Tony, C.; Bozek, J. D.; Saykally, R. J. Characterization of hydrogen bond acceptor molecules at the water surface using near-edge x-ray absorption fine-structure spectroscopy and density functional theory. *J. Phys.: Condens. Matter* **2002**, *14*, L221.

(3) Nooijen, M.; Bartlett, R. J. Description of core excitation spectra by the open-shell electron-attachment equation-of-motion coupled cluster method. *J. Chem. Phys.* **1995**, *102*, 6735−6756.

(4) Sheehy, J. A.; Gil, T. J.; Winstead, C. L.; Farren, R. E.; Langhoff, P. W. Correlation of molecular valence and K-shell photoionization resonances with bond lengths. *J. Chem. Phys.* **1989**, *91*, 1796−1812.

(5) Kolczewski, C.; Puttner, R.; Plashkevych, O.; Ãgren, H.; Staemmler, V.; Martins, M.; Snell, G.; Schlachter, A. S.; Sant'Anna, M.; Kaindl, G.; Pettersson, L. G. M. Detailed study of pyridine at the Ca1s and Na1s ionization thresholds: The influence of the vibrational fine structure. *J. Chem. Phys.* **2001**, *115*, 6426−6437.

(6) Ãgren, H.; Carravetta, V.; Vahtras, O.; Pettersson, L. G. M. Direct, atomic orbital, static exchange calculations of photoabsorption spectra of large molecules and clusters. *Chem. Phys. Lett.* **1994**, *222*, 75−81.

(7) Butscher, W.; Buenker, R. J.; Peyerimhoff, S. D. All-electron CI calculations for core-ionized, core-valence excited and shake-up states of N_2. *Chem. Phys. Lett.* **1977**, *52*, 449−456.

(8) Barth, A.; Buenker, R. J.; Peyerimhoff, S. D.; Butscher, W. Theoretical study of the core-ionized and various core-excited and shake-up states of acetylene and ethylene by ab initio MRD-CI methods. *Chem. Phys.* **1980**, *46*, 149−164.

(9) Rehr, J. J.; Albers, R. C. Theoretical approaches to x-ray absorption fine structure. *Rev. Mod. Phys.* **2000**, *72*, 621−654.

(10) Schirmer, J. Beyond the random-phase approximation: A new approximation scheme for the polarization propagator. *Phys. Rev. A* **1982**, *26*, 2395−2416.

(11) Plekan, O.; Feyer, V.; Richter, R.; Coreno, M.; de Simone, M.; Prince, K. C.; Trofimov, A. B.; Gromov, E. V.; Zaytseva, I. L.; Schirmer, J. A theoretical and experimental study of the near edge X-ray absorption fine structure (NEXAFS) and X-ray photoelectron spectra (XPS) of nucleobases: Thymine and adenine. *Chem. Phys.* **2008**, *347*, 360−375.
(12) Stanton, J. F.; Bartlett, R. J. The equation of motion coupled-cluster method. A systematic biorthogonal approach to molecular excitation energies, transition probabilities, and excited state properties. *J. Chem. Phys.* **1993**, *98*, 7029−7039.
(13) Koch, H.; Jørgensen, P. Coupled cluster response functions. *J. Chem. Phys.* **1990**, *93*, 3333−3344.
(14) Monkhorst, H. J. Calculation of properties with the coupled-cluster method. *Int. J. Quantum Chem.* **1977**, *12*, 421−432.
(15) Kuramoto, K.; Ehara, M.; Nakatsuji, H. Theoretical fine spectroscopy with symmetry adapted cluster-configuration interaction general-R method: First-row K-shell ionizations and their satellites. *J. Chem. Phys.* **2005**, *122*, 014304.
(16) Ohtsuka, Y.; Nakatsuji, H. Inner-shell ionizations and satellites studied by the open-shell reference symmetry-adapted cluster/symmetry-adapted cluster configuration-interaction method. *J. Chem. Phys.* **2006**, *124*, 054110.
(17) Besley, N. A. Equation of motion coupled cluster theory calculations of the X-ray emission spectroscopy of water. *Chem. Phys. Lett.* **2012**, *542*, 42−46.
(18) Coriani, S.; Christiansen, O.; Fransson, T.; Norman, P. Coupled-cluster response theory for near-edge x-ray-absorption fine structure of atoms and molecules. *Phys. Rev. A* **2012**, *85*, 022507.
(19) Brabec, J.; Bhaskaran-Nair, K.; Govind, N.; Pittner, J.; Kowalski, K. Communication: Application of state-specific multireference coupled cluster methods to core-level excitations. *J. Chem. Phys.* **2012**, *137*, 171101.
(20) Pittner, J.; Nachtigall, P.; Carsky, P.; Masik, J.; Hubac, I. Assessment of the single-root multireference Brillouin−Wigner coupled- cluster method: Test calculations on CH_2, SiH_2, and twisted ethylene. *J. Chem. Phys.* **1999**, *110*, 10275−10282.
(21) Mahapatra, U. S.; Datta, B.; Mukherjee, D. A state-specific multi-reference coupled cluster formalism with molecular applications. *Mol. Phys.* **1998**, *94*, 157−171.
(22) Sen, S.; Shee, A.; Mukherjee, D. A study of the ionisation and excitation energies of core electrons using a unitary group adapted state universal approach. *Mol. Phys.* **2013**, *111*, 2625−2639.
(23) Maitra, R.; Sinha, D.; Mukherjee, D. Unitary group adapted state-specific multi-reference coupled cluster theory: Formulation and pilot numerical applications. *J. Chem. Phys.* **2012**, *137*, 024105.
(24) Sen, S.; Shee, A.; Mukherjee, D. Formulation and implementation of a unitary group adapted state universal multi-reference coupled cluster (UGA-SUMRCC) theory: Excited and ionized state energies. *J. Chem. Phys.* **2012**, *137*, 074104.
(25) The UGA-QFMRCC method is capable of core excitation energy as direct difference of energy
(26) Kaldor, U.; Haque, A. Open-shell coupled-cluster method: Direct calculation of excitation energies. *Chem. Phys. Lett.* **1986**, *128*, 45−48.
(27) Pal, S. Fock space multi-reference coupled-cluster method for energies and energy derivatives. *Mol. Phys.* **2010**, *108*, 3033−3042.
(28) Pal, S.; Rittby, M.; Bartlett, R. J.; Sinha, D.; Mukherjee, D. Multireference coupled-cluster methods using an incomplete model space: Application to ionization potentials and excitation energies of formaldehyde. *Chem. Phys. Lett.* **1987**, *137*, 273−278.
(29) Pal, S.; Rittby, M.; Bartlett, R. J.; Sinha, D.; Mukherjee, D. Molecular applications of multireference coupled-cluster methods using an incomplete model space: Direct calculation of excitation energies. *J. Chem. Phys.* **1988**, *88*, 4357−4366.
(30) Vaval, N.; Ghose, K. B.; Pal, S.; Mukherjee, D. Fock-space multireference coupled-cluster theory. fourth-order corrections to the ionization potential. *Chem. Phys. Lett.* **1993**, *209*, 292−298.
(31) Vaval, N.; Pal, S.; Mukherjee, D. Fock space multireference coupled cluster theory: noniterative inclusion of triples for excitation energies. *Theor. Chem. Acc.* **1998**, *99*, 100−105.
(32) Musial, M.; Kucharski, S.; Zerzucha, P.; Kus, T.; Bartlett, R. J. Excited and ionized states of the ozone molecule with full triples coupled cluster methods. *J. Chem. Phys.* **2009**, *131*, 194104.
(33) Vaval, N.; Pal, S. Adiabatic states of ozone using Fock space multireference coupled cluster method. *J. Chem. Phys.* **1999**, *111*, 4051−4055.
(34) Schucan, T. H.; Weidenmuller, H. A. The effective interaction in nuclei and its perturbation expansion: An algebraic approach. *Ann. Phys.* **1972**, *73*, 108−135.
(35) Schucan, T. H.; Weidenmuller, H. A. Perturbation theory for the effective interaction in nuclei. *Ann. Phys.* **1973**, *76*, 483−509.
(36) Baker, H.; Robb, M. A.; Slattery, Z. The method of minimized iterations in multi-reference (effective hamiltonian) perturbation theory. *Mol. Phys.* **1981**, *44*, 1035−1042.
(37) Sten, S.; Ingvar, L.; Ann-Marie, M. Numerical Many-Body Perturbation Calculations on Be-like Systems Using a Multi-Configurational Model Space. *Phys. Scr.* **1980**, *21*, 351.
(38) Kaldor, U. Intruder states and incomplete model spaces in multireference coupled-cluster theory: The $2p^2$ states of Be. *Phys. Rev. A* **1988**, *38*, 6013−6016.
(39) Malrieu, J. P.; Durand, P.; Daudey, J. P. Intermediate Hamiltonians as a new class of effective Hamiltonians. *J. Phys. A: Math. Gen.* **1985**, *18*, 809.
(40) Landau, A.; Eliav, E.; Kaldor, U., Intermediate Hamiltonian Fock-space coupled-cluster method. In *Advances in Quantum Chemistry*; Sabin, J. R., Bäandas, E., Eds.; Academic Press: 2001; Vol. *39*, pp 171−188.
(41) Landau, A.; Eliav, E.; Kaldor, U. Intermediate Hamiltonian Fock-space coupled-cluster method. *Chem. Phys. Lett.* **1999**, *313*, 399−403.
(42) Meissner, L. Fock-space coupled-cluster method in the intermediate Hamiltonian formulation: Model with singles and doubles. *J. Chem. Phys.* **1998**, *108*, 9227−9235.
(43) Musial, M.; Meissner, L.; Kucharski, S. A.; Bartlett, R. J. Molecular applications of the intermediate Hamiltonian Fock-space coupled-cluster method for calculation of excitation energies. *J. Chem. Phys.* **2005**, *122*, 224110.
(44) Musial, M.; Meissner, L. The fock-space coupled-cluster method in the calculation of excited state properties. *Collect. Czech. Chem. Commun.* **2005**, *70*, 811−825.
(45) Meissner, L.; Malinowski, P. Intermediate Hamiltonian formulation of the valence-universal coupled-cluster method for atoms. *Phys. Rev. A* **2000**, *61*, 062510.
(46) Meissner, L.; Nooijen, M. Effective and intermediate Hamiltonians obtained by similarity transformations. *J. Chem. Phys.* **1995**, *102*, 9604−9614.
(47) Malinowski, P.; Meissner, L.; Nowaczyk, A. Application of the intermediate Hamiltonian valence-universal coupled-cluster method to the magnesium atom. *J. Chem. Phys.* **2002**, *116*, 7362−7371.
(48) Meissner, L.; Malinowski, P.; Gryniakow, J. Approximate evaluation of the effect of three-body cluster operators in the valence-universal coupled-cluster excitation energy calculations for Be and Mg. *J. Phys. B* **2004**, *37*, 2387.
(49) Musial, M.; Bartlett, R. J. Multi-reference Fock space coupled-cluster method in the intermediate Hamiltonian formulation for potential energy surfaces. *J. Chem. Phys.* **2011**, *135*, 044121.
(50) Sinha, D.; Mukhopadhyay, S. K.; Chaudhuri, R.; Mukherjee, D. The eigenvalue-independent partitioning technique in Fock space: An alternative route to open-shell coupled-cluster theory for incomplete model spaces. *Chem. Phys. Lett.* **1989**, *154*, 544−549.
(51) Musial, M.; Bartlett, R. J. Benchmark calculations of the Fock-space coupled cluster single, double, triple excitation method in the intermediate Hamiltonian formulation for electronic excitation energies. *Chem. Phys. Lett.* **2008**, *457*, 267−270.

(52) Musial, M.; Bartlett, R. J. Intermediate Hamiltonian Fock-space multireference coupled-cluster method with full triples for calculation of excitation energies. *J. Chem. Phys.* **2008**, *129*, 044101.
(53) Musial, M.; Bartlett, R. J. Spin-free intermediate Hamiltonian Fock space coupled-cluster theory with full inclusion of triple excitations for restricted Hartree Fock based triplet states. *J. Chem. Phys.* **2008**, *129*, 244111.
(54) Musial, M. Efficient realization of the Fock-space coupled-cluster method with connected triple excitations. *Chem. Phys. Lett.* **2009**, *470*, 358−362.
(55) Musial, M.; Bartlett, R. J. Multireference Fock-space coupled-cluster and equation-of-motion coupled-cluster theories: The detailed interconnections. *J. Chem. Phys.* **2008**, *129*, 134105.
(56) Musial, M. Multireference Fock space coupled cluster method in the effective and intermediate Hamiltonian formulation for the (2,0) sector. *J. Chem. Phys.* **2012**, *136*, 044121.
(57) Mášik, J.; Hubač, I., Multireference Brillouin-Wigner Coupled-Cluster Theory. Single-root approach. In *Advances in Quantum Chemistry*; Sabin, J. R., Zerner, M. C., Brändas, E., Wilson, S., Maruani, J., Smeyers, Y. G., Grout, P. J., McWeeny, R., Eds.; Academic Press: Waltham, MA, 1998; Vol. *31*, pp 75−104.
(58) Ravishankara, A. R.; Daniel, J. S.; Portmann, R. W. Nitrous Oxide (N2O): The Dominant Ozone-Depleting Substance Emitted in the 21st Century. *Science* **2009**, *326*, 123−125.
(59) Evangelista, F. A.; Simmonett, A. C.; Allen, W. D.; Schaefer, H. F., III; Gauss, J. Triple excitations in state-specific multireference coupled cluster theory: Application of Mk-MRCCSDT and Mk-MRCCSDT-n methods to model systems. *J. Chem. Phys.* **2008**, *128*, 124104−13.
(60) Evangelista, F. A.; Gauss, J. An orbital-invariant internally contracted multireference coupled cluster approach. *J. Chem. Phys.* **2011**, *134*, 114102−15.
(61) Evangelista, F. A.; Allen, W. D.; Schaefer, H. F., III Coupling term derivation and general implementation of state-specific multi-reference coupled cluster theories. *J. Chem. Phys.* **2007**, *127*, 024102−17.
(62) Hanrath, M. Higher excitations for an exponential multi-reference wavefunction Ansatz and single-reference based multi-reference coupled cluster Ansatz: Application to model systems H_4, P_4, and BeH_2. *J. Chem. Phys.* **2008**, *128*, 154118−10.
(63) Hanrath, M. An exponential multireference wave-function Ansatz. *J. Chem. Phys.* **2005**, *123*, 084102−12.
(64) Hanauer, M.; Kohn, A. Pilot applications of internally contracted multireference coupled cluster theory, and how to choose the cluster operator properly. *J. Chem. Phys.* **2011**, *134*, 204111−20.
(65) Balkova, A.; Kucharski, S. A.; Meissner, L.; Bartlett, R. J. The multireference coupled-cluster method in Hilbert space: An incomplete model space application to the LiH molecule. *J. Chem. Phys.* **1991**, *95*, 4311−4316.
(66) Balkova, A.; Bartlett, R. J. A multireference coupled-cluster study of the ground state and lowest excited states of cyclobutadiene. *J. Chem. Phys.* **1994**, *101*, 8972−8987.
(67) Mukherjee, D.; Pal, S. Use of Cluster Expansion Methods in the Open-Shell Correlation Problem. In *Advances in Quantum Chemistry*; Academic Press: Waltham, MA, 1989; Vol. *20*, pp 291−373.
(68) Mukherjee, D. Aspects of linked cluster expansion in general model space many-body perturbation and coupled-cluster theory. *Int. J. Quantum Chem.* **1986**, *30*, 409−435.
(69) Shavitt, I.; Bartlett, R. J. *Many-body methods in chemistry and physics: MBPT and coupled-cluster theory*. Cambridge University Press: Cambridge, U.K., 2009; pp 490−495.
(70) Stanton, J. F.; Gauss, J. Analytic energy derivatives for ionized states described by the equation-of-motion coupled cluster method. *J. Chem. Phys.* **1994**, *101*, 8938−8944.
(71) Nooijen, M.; Bartlett, R. J. Equation of motion coupled cluster method for electron attachment. *J. Chem. Phys.* **1995**, *102*, 3629−3647.
(72) Gupta, J.; Vaval, N.; Pal, S. A Lagrange multiplier approach for excited state properties through intermediate Hamiltonian formulation of Fock space multireference coupled-cluster theory. *J. Chem. Phys.* **2013**, *139*, 074108.
(73) Davidson, E. R. The iterative calculation of a few of the lowest eigenvalues and corresponding eigenvectors of large real-symmetric matrices. *J. Comput. Phys.* **1975**, *17*, 87−94.
(74) Hirao, K.; Nakatsuji, H. A generalization of the Davidson's method to large nonsymmetric eigenvalue problems. *J. Comput. Phys.* **1982**, *45*, 246−254.
(75) Dunning, T. H. Gaussian basis sets for use in correlated molecular calculations. I. The atoms boron through neon and hydrogen. *J. Chem. Phys.* **1989**, *90*, 1007−1023.
(76) Woon, D. E.; Dunning, T. H. Gaussian basis sets for use in correlated molecular calculations. V. Core-valence basis sets for boron through neon. *J. Chem. Phys.* **1995**, *103*, 4572−4585.
(77) Bag, A.; Manohar, P. U.; Vaval, N.; Pal, S. First- and second-order electrical properties computed at the FSMRCCSD level for excited states of closed-shell molecules using the constrained-variational approach. *J. Chem. Phys.* **2009**, *131*, 024102.
(78) Schmidt, M. W.; Baldridge, K. K.; Boatz, J. A.; Elbert, S. T.; Gordon, M. S.; Jensen, J. H.; Koseki, S.; Matsunaga, N.; Nguyen, K. A.; Su, S.; Windus, T. L.; Dupuis, M.; Montgomery, J. A. General atomic and molecular electronic structure system. *J. Comput. Chem.* **1993**, *14*, 1347−1363.
(79) Stanton, J. F.; Gauss, J.; Harding, M. E.; Szalay, P. G. *CFOUR. Coupled-Cluster techniques for Computational Chemistry*; Universität Mainz: Mainz, Germany, 2010; http://www.cfour.de.
(80) See SI at for the cartesian coordinates of geometry used for all the molecules.
(81) Schirmer, J.; Trofimov, A. B.; Randall, K. J.; Feldhaus, J.; Bradshaw, A. M.; Ma, Y.; Chen, C. T.; Sette, F. K-shell excitation of the water, ammonia, and methane molecules using high-resolution photoabsorption spectroscopy. *Phys. Rev. A* **1993**, *47*, 1136−1147.
(82) Nooijen, M.; Bartlett, R. J. Similarity transformed equation-of-motion coupled-cluster theory: Details, examples, and comparisons. *J. Chem. Phys.* **1997**, *107*, 6812−6830.
(83) Chen, C. T.; Ma, Y.; Sett, F. K-shell phoro absorption spectra of N_2 molecule. *Phys. Rev. A* **1989**, *40*, 6737−6740.
(84) Barth, A.; Schirmer, J. Theoretical core-level excitation spectra of N_2 and CO by a new polarisation propagator method. *J. Phys. B* **1985**, *18*, 867.
(85) Ehara, M.; Nakatsuji, H. Geometry Relaxations After Inner-Shell Excitations and Ionizations. *Collect. Czech. Chem. Commun.* **2008**, *73*, 771−785.
(86) Puttner, R.; Dominguez, I.; Morgan, T. J.; Cisneros, C.; Fink, R. F.; Rotenberg, E.; Warwick, T.; Domke, M.; Kaindl, G.; Schlachter, A. S. Vibrationally resolved O 1s core excitation spectra of CO and NO. *Phys. Rev. A* **1999**, *59*, 3415−3423.
(87) Domke, M.; Xue, C.; Puschmann, A.; Mandel, T.; Hudson, E.; Shirley, D. A.; Kaindl, G. Carbon and oxygen K-edge photoionization of the CO molecule. *Chem. Phys. Lett.* **1990**, *173*, 122−128.
(88) Tronc, M.; King, G. C.; Read, F. H. Carbon K-shell excitation in small molecules by high-resolution electron impact. *J. Phys. B* **1979**, *12*, 137.
(89) Remmers, G.; Domke, M.; Puschmann, A.; Mandel, T.; Xue, C.; Kaindl, G.; Hudson, E.; Shirley, D. A. High-resolution K-shell photoabsorption in formaldehyde. *Phys. Rev. A* **1992**, *46*, 3935−3944.